III. 研究成果の刊行に関する一覧表

研究成果の刊行に関する一覧表レイアウト

1. 論文発表

発表者氏名	論文タイトル名	発表誌名	巻・号	ページ	出版年
Kunishima S, Kashiwagi H, Otsu M, Takayama N, Eto K, Onodera M, Miyajima Y, Takamatsu Y, Suzumiya J, Matsubara K, Tomiyama Y, Saito H.	Heterozygous *ITGA2B* R995W mutation inducing constitutive activation of the αIIbβ3 receptor affects proplatelet formation and causes congenital macrothrombocytopenia.	***Blood***	117	5479-84	2011
Takeyama M, Uchida Y, Arai I, Kamamoto T, Nishikubo T, Kanehiro H, Sado T, Kunishima S, Takahashi Y:	Neonatal case of transient abnormal myelopoiesis in Down's syndrome treated by Inchinkoto.	***Pediatr Int***	53	1093-6	2011
Flatland B, Kunishima S.	Successful immunostaining demonstrates abnormal intracytoplasmic *MYH9* protein (NMMHC-IIA) in neutrophils of a dog with May-Hegglin Anomaly.	***Vet Clin Pathol***	40	409-10	2011
Tsuburaya R, Uematsu M, Kikuchi A, Hino-Fukuyo N, Kunishima S, Kato M, Haginoya K, Tsuchiya S.	Unusual ribbon-like periventricular heterotopia with congenital cataracts in a Japanese girl.	**Am J Med Genet**	158 A	674-7	2012
Shiota M, Kunishima S, Hamabata T, Nakata M,	Early diagnosis improves the quality of life in	***Pediatr Blood***	58	314-5	2012

Hata D.	*MYH9* disorder.	***Cancer***			
Hao J, Kunishima S, Guo X, Hu R, Gao W.	A large family with *MYH9* disorder caused by E1841K mutation, suffering from serious kidney and hearing impairment and cataracts.	***Ann Hematol***			in press
Uyeda T, Echizenya T, Eto S, Otani K, Sato T, Takahashi T, Ito E, Yonesaka S, Kunishima S.	A patient with Adams-Oliver Syndrome and familial *MYH9* mutation.	***Pediatr Int***			in press

総説原稿

著者氏名	論文タイトル	編集者(書籍)	書籍名	ページ	出版年
國島伸治	先天性巨大血小板症の鑑別診断		血栓止血誌	2巻:100-6	2011
國島伸治	先天性巨大血小板症の原因となるGPIIb/IIIa異常	高久史麿、他	Annual Review 2012 血液	p181-191	2012
國島伸治、齋藤英彦	May-Hegglin anomaly		標本に学ぶ血液疾患症例	p276-80	2012

IV. 研究成果の刊行物・別刷

blood

2011 117: 5479-5484
Prepublished online March 31, 2011;
doi:10.1182/blood-2010-12-323691

Heterozygous *ITGA2B* R995W mutation inducing constitutive activation of the αIIbβ3 receptor affects proplatelet formation and causes congenital macrothrombocytopenia

Shinji Kunishima, Hirokazu Kashiwagi, Makoto Otsu, Naoya Takayama, Koji Eto, Masafumi Onodera, Yuji Miyajima, Yasushi Takamatsu, Junji Suzumiya, Kousaku Matsubara, Yoshiaki Tomiyama and Hidehiko Saito

Blood (print ISSN 0006-4971, online ISSN 1528-0020), is published weekly by the American Society of Hematology, 2021 L St, NW, Suite 900, Washington DC 20036.

Brief report

Heterozygous *ITGA2B* R995W mutation inducing constitutive activation of the αIIbβ3 receptor affects proplatelet formation and causes congenital macrothrombocytopenia

Shinji Kunishima,[1] Hirokazu Kashiwagi,[2] Makoto Otsu,[3] Naoya Takayama,[3] Koji Eto,[3] Masafumi Onodera,[4] Yuji Miyajima,[5] Yasushi Takamatsu,[6] Junji Suzumiya,[7] Kousaku Matsubara,[8] Yoshiaki Tomiyama,[2,9] and Hidehiko Saito[10]

[1]Department of Advanced Diagnosis, Clinical Research Center, National Hospital Organization Nagoya Medical Center, Nagoya, Japan; [2]Department of Hematology and Oncology, Graduate School of Medicine, Osaka University, Osaka, Japan; [3]Division of Stem Cell Therapy, Center for Stem Cell and Regenerative Medicine, Institute of Medical Science, University of Tokyo, Tokyo, Japan; [4]Department of Genetics, National Research Institute for Child Health and Development, Tokyo, Japan; [5]Department of Pediatrics, Anjo Kosei Hospital, Anjo, Japan; [6]Department of Medical Oncology, Hematology and Infectious Disease, Fukuoka University, Fukuoka, Japan; [7]Shimane University Hospital Cancer Center, Shimane, Japan; [8]Department of Pediatrics, Nishi-Kobe Medical Center, Kobe, Japan; [9]Department of Blood Transfusion, Osaka University Hospital, Osaka, Japan; and [10]Nagoya Central Hospital, Nagoya, Japan

Congenital macrothrombocytopenia is a genetically heterogeneous group of rare disorders. αIIbβ3 has not been implicated in these conditions. We identified a novel, conserved heterozygous *ITGA2B* R995W mutation in 4 unrelated families. The surface expression of platelet αIIbβ3 was decreased to 50% to 70% of control. There was spontaneous PAC-1 and fibrinogen binding to resting platelets without CD62p expression. The activation state of αIIbβ3 in 293T cells was higher for αIIb-W995 than for β3-H723 but was weaker than for β3-N562. FAK was spontaneously phosphorylated in αIIb-W995/β3-transfected 293T cells. These results indicate that αIIb-W995/β3 has a constitutive, activated conformation but does not induce platelet activation. αIIb-W995/β3-transfected CHO cells developed membrane ruffling and abnormal cytoplasmic protrusions. The increased size and decreased number of proplatelet tips in αIIb-W995/β3-transduced mouse fetal liver-derived megakaryocytes indicate defective proplatelet formation. We propose that activating mutations in *ITGA2B* and *ITGB3* represent the etiology of a subset of congenital macrothrombocytopenias. (*Blood.* 2011;117(20):5479-5484)

Introduction

Congenital macrothrombocytopenia is a genetically heterogeneous group of rare disorders.[1-4] The most frequent forms include *MYH9* disorders and Bernard-Soulier syndrome. In approximately half of cases of congenital macrothrombocytopenia, the pathogenesis remains unknown; thus, a definite diagnosis is unavailable. Glanzmann thrombasthenia is the most common congenital platelet disorder caused by qualitative or quantitative abnormality of the integrin αIIbβ3, in which the platelet counts and morphology are normal.[5] However, *ITGA2B* R995Q mutation has been reported in a patient with Glanzmann thrombasthenia-like phenotype and macrothrombocytopenia.[6,7] Recently, heterozygous *ITGB3* mutations were found in patients with congenital macrothrombocytopenia.[8-10] We report here a novel, conserved heterozygous *ITGA2B* R995W mutation in 4 unrelated families.

Methods

Patients

Twenty-seven patients with congenital macrothrombocytopenia, in whom *MYH9* disorders, heterozygous and homozygous Bernard-Soulier syndrome, type 2B von Willebrand disease, and *TUBB1* mutations were excluded, underwent mutational analysis of *ITGA2B* and *ITGB3*. Fifty-five consecutive patients were prospectively analyzed for the surface expression of platelet αIIbβ3. Written informed consent was obtained from all patients or their parents in accordance with the Declaration of Helsinki. Institutional review boards of Nagoya Medical Center and each of the participating institutions/hospitals approved this study.

Genetic analysis

The entire coding sequence of exons and exon-intron boundaries of *ITGA2B* (supplemental Table 1, available on the *Blood* Web site; see the Supplemental Materials link at the top of the online article) and *ITGB3* was amplified by polymerase chain reaction and sequenced. The disease-associated *ITGA2B* haplotype was determined by cloning and sequencing the polymerase chain reaction products.

Platelet glycoprotein analysis

Flow cytometry and immunoblotting were performed as described previously.[11,12] The activation state of αIIbβ3 was evaluated by the binding of the ligand-mimetic antibody PAC-1 (BD Biosciences) and FITC-labeled fibrinogen.[13]

Cloning, mutagenesis, and retroviral transduction

ITGA2B and *ITGB3* sequences were amplified from the patient's platelet cDNA and cloned into pcDNA3.1 (Invitrogen). T562N[13] and D723H[8] were introduced into *ITGB3* cDNA using site-directed mutagenesis. *ITGA2B* and *ITGB3* expression plasmids were cotransfected into 293T and CHO cells.

Submitted December 7, 2010; accepted March 18, 2011. Prepublished online as *Blood* First Edition paper, March 31, 2011; DOI 10.1182/blood-2010-12-323691.

The online version of this article contains a data supplement.

The publication costs of this article were defrayed in part by page charge payment. Therefore, and solely to indicate this fact, this article is hereby marked "advertisement" in accordance with 18 USC section 1734.

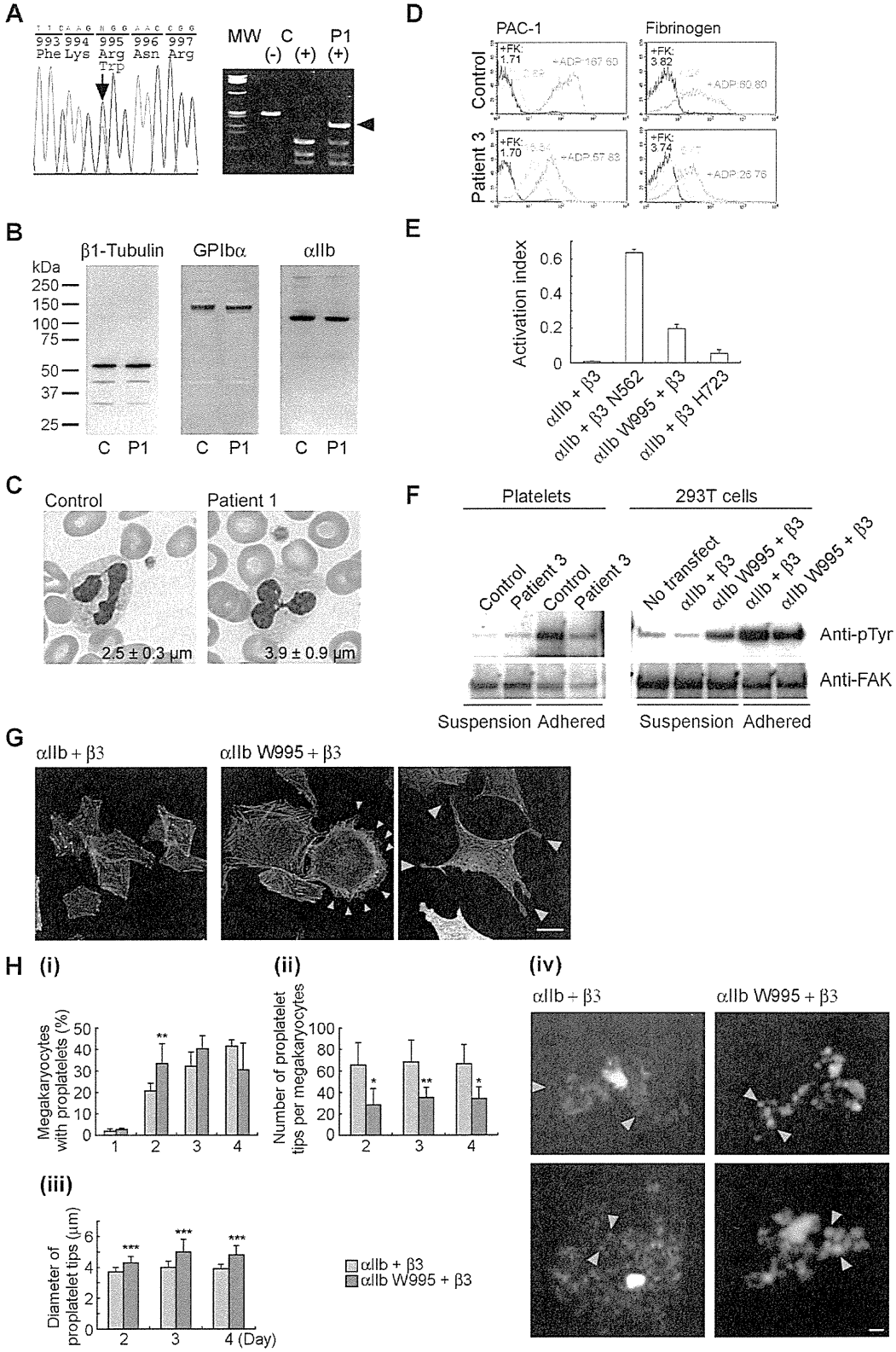

Figure 1. Platelet morphology and biochemical, genetic, and functional analyses of *ITGA2B* R995W mutation. (A; left) DNA sequence analysis of *ITGA2B*. The entire coding regions of the patients' *ITGA2B* were amplified from genomic DNA by the polymerase chain reaction, and amplified DNA fragments were subjected to direct cycle sequence analysis. A C to T transition at nucleotide 3077, changing Arg995 to Trp (R995W), was detected. Nucleotide numbering for *ITGA2B* cDNA is according to Poncz et al.[18] The arrow shows the position of the substitution. (Right) Allele-specific restriction analysis. DNA fragments amplified using primers 2Bg305/303 (supplemental Table 1) were digested with BspACI (SibEnzyme), electrophoresed on 2% agarose gels, and stained with ethidium bromide. The 3077C > T substitution abolishes a recognition site for BspACI, generating a new 231-bp band (arrowhead). The mutation was not found in 108 healthy controls or in the SNP database (www.ncbi.nlm.nih.gov/SNP). MW indicates HaeIII digest of ΦX 174 DNA; C, control; and P1, patient 1. (B) Immunoblot analysis of platelets. Triton X-100-soluble platelet lysates were separated by sodium dodecyl sulfate-polyacrylamide gel electrophoresis on 4% to 12% gradient acrylamide slab gels (Invitrogen) and electroblotted onto polyvinylidine difluoride membranes. The blots were incubated with anti-β1 tubulin antibody NB2301,[19] anti-GPIbα antibody PL524 (Takara), and anti-αIIb antibody SZ22 (Beckman-Coulter) and reacted with horseradish peroxidase-conjugated secondary antibody. The bound antibodies were visualized using an enhanced chemiluminescent substrate. C indicates control; and P1, patient 1.

Transfected cells were subjected to flow cytometry, FAK phosphorylation, and spreading assay.[13,14]

ITGA2B and *ITGB3* cDNAs were inserted upstream of internal ribosome entry site (IRES)-enhanced green fluorescent protein (EGFP) and IRES-Kusabira-Orange in the retroviral vector pGCDNsamIRES/EGFP and pGCDNsamIRES/huKO, respectively.[15,16] Each plasmid was transfected into 293gp packaging cells with a vesicular stomatitis virus G expression plasmid. Supernatants were used for the transduction of 293gpg producer cells harboring a tetracycline-inducible vesicular stomatitis virus G expression cassette,[17] and virus-bearing supernatant was harvested under tetracycline-deficient conditions.

Mouse fetal liver cells were harvested from embryonic day 13.5 embryos and cultured in Dulbecco modified Eagle medium supplemented with 10% fetal calf serum and 50 ng/mL human thrombopoietin. The next day, cells were infected with retroviruses expressing *ITGA2B* and *ITGB3* on recombinant human fibronectin fragment CH-296 (RetroNectin, Takara)-coated plates. After transduction, proplatelet formation was monitored for the next 4 days on EGFP and Kusabira-Orange double-positive megakaryocytes in suspension by inverted fluorescence microscopy. The Experimental Animal Committee of Nagoya Medical Center approved the animal studies.

Results and discussion

We searched for *ITGA2B* and *ITGB3* mutations in 27 patients with macrothrombocytopenia and identified a novel, conserved heterozygous *ITGA2B* R995W mutation in one patient (patient 1; Figure 1A). The decreased surface expression of platelet αIIbβ3 prompted us to prospectively screen its expression by flow cytometry. We detected decreased αIIbβ3 expression level (50%-70% of control) in 3 of 55 consecutive patients with macrothrombocytopenia of unknown etiology (patients 2-4 in Table 1). Immunoblotting showed a normal electrophoretic mobility of αIIb, but the total expression level relative to β1-tubulin was decreased to 0.7 (Figure 1B; Table 1). Sequence analysis identified the same heterozygous *ITGA2B* R995W mutation. In total, we identified 11 patients in 4 unrelated Japanese families. In each family, the disease-associated *ITGA2B* haplotype was unique, indicating independent occurrence (supplemental Table 2). Patients had larger platelets, approximately 30% increase of control, and moderate thrombocytopenia (Figure 1C; Table 1). These results indicate that macrothrombocytopenia shows a dominant inheritance.

Bleeding tendency was absent or mild (eg, patient 1 had undergone total colectomy without platelet transfusion). Platelet aggregation induced by adenosine diphosphate and collagen was reduced, although the bleeding time was within the normal limit (Table 1). Platelet spreading on immobilized fibrinogen was partially impaired: the number of fully spread platelets was decreased (supplemental Figure 1). These findings indicate that patients are asymptomatic or exhibit a marginal bleeding tendency and that the clinical and laboratory phenotype is distinct from Glanzmann thrombasthenia.

There was spontaneous PAC-1 binding to resting patients' platelets as well as to αIIb-W995/β3-transfected 293T cells. Although fibrinogen did not bind to platelets in whole blood, increased fibrinogen binding to the washed platelets was observed (Figure 1D; supplemental Figure 2). The activation state, quantified as an activation index in 293T cells, was higher for αIIb-W995 than for β3-H723 but was weaker than that for a strong activating mutant, β3-N562[13](Figure 1E). CD62p expression was absent on the resting platelets (supplemental Figure 2). Spontaneously phosphorylated FAK, a downstream effector of integrin signaling, was not evident in resting platelets in suspension, probably because of low expression level of abnormal αIIbβ3 receptor. However, FAK phosphorylation occurred in αIIb-W995/β3-transfected 293T cells in suspension, indicating constitutively activated αIIbβ3 (Figure 1F). These results indicate that R995W mutation changes αIIbβ3 to a constitutively, albeit partially, activated conformation, but does not induce platelet activation.

αIIb-R995 forms a salt bridge with β3-D723 in the membrane-proximal region and maintains the inactive conformation of the αIIbβ3.[20,21] Disruption of the interaction because of partially activated αIIb/β3-H723 or αIIb/β3-A723 mutants but not fully activated mutants, such as αIIb/β3-N562, was reported to cause microtubule-dependent abnormal proplatelet-like cytoplasmic extensions in megakaryocytes and CHO cells.[8,22] We found that

Figure 1. (continued) (C) Platelet morphology. Peripheral blood smears were stained with May-Grünwald-Giemsa for a normal control and patient 1 (original magnification, × 1000). The patient showed giant platelets with morphologically normal leukocytes. The number in each panel shows the mean platelet size (n = 200). Images were obtained using a BX50 microscope with a 100×/1.35 numeric aperture oil objective (Olympus). Images of the slides were acquired using a DP70 digital camera and DP manager software Version 1.2.1.107 (Olympus). (D) Activation state of platelet αIIbβ3. Washed platelets from patient 3 were resuspended in Tyrode buffer (137mM NaCl, 2.7mM KCl, 1.0mM $MgCl_2$, 3.3mM NaH_2PO_4, 3.8mM N-2-hydroxyethylpiperazine-N′-2-ethanesulfonic acid, 0.1% glucose, 0.1% bovine serum albumin, pH 7.4) and incubated with fluorescein isothiocyanate-conjugated PAC-1 or 125 μg/mL fluorescein isothiocyanate-labeled fibrinogen in the presence or absence of 10μM FK633 (αIIbβ3-specific peptidomimetic antagonist: black lines) or 10μM adenosine diphosphate (blue lines), and analyzed by flow cytometry. Numbers indicate the mean fluorescence intensity. Results are representative of 2 independent experiments. (E) Quantitation of the αIIbβ3 activation state. The activation state of αIIbβ3 was quantified as an activation index on transiently transfected 293T cells. The activation index was higher for αIIb-W995 than for β3-H723 but was weaker than for an activating mutant β3-N562. Activation index = (a − b)/(c − b), in which a is the mean fluorescence intensity of PAC-1 binding with buffer, b is the mean fluorescence intensity in the presence of FK633, and c is the mean fluorescence intensity in the presence of PT25–2 (anti-αIIbβ3 antibody, which induces the active conformation of αIIbβ3). Data are mean plus or minus SE (n = 3). (F) FAK phosphorylation. Washed platelets from patient 3 (left) or transiently transfected 293T cells (right) were incubated in suspension or seeded onto 100-μg/mL fibrinogen-coated plastic dishes for 1 hour. Cells were washed with phosphate-buffered saline and lysed with 1% Triton X-100 and 1mM sodium vanadate. FAK was immunoprecipitated from the lysates with anti-FAK antibody FAK(C903; Santa Cruz Biotechnology) and protein G-Sepharose, and phosphotyrosine was detected with the antiphosphotyrosine antibody 4G10 (Millipore). Note that 300-μg and 150-μg lysates from suspension and adhered platelets, respectively, and 200-μg lysates from suspension and adhered transfected 293T cells were used for immunoprecipitation analysis. To monitor the loading of gel lanes, the membrane was stripped and reprobed with the anti-FAK antibody FAK(A17; Santa Cruz Biotechnology). Results are representative of 2 and 3 independent experiments for platelets and transfected cells, respectively. (G) Abnormal cytoplasmic protrusions in αIIb-W995/β3-transfected CHO cells. Stably transfected CHO cells were seeded onto 100 μg/mL fibrinogen-coated glass coverslips and incubated for 2 hours at 37°C. Cells were fixed with 3.7% formaldehyde and permeabilized with 0.2% Triton X-100. Coverslips were then stained with anti-CD41a antibody HIP8 (BD Biosciences) followed by Alexa-488-labeled goat antimouse IgG (Invitrogen) and tetramethylrhodamine isothiocyanate-phalloidin (Sigma-Aldrich). Images were obtained using a confocal microscope with a Plan-Apochromat 63×/1.4 oil DIC objective lens LSM5Pascal (Carl Zeiss). Arrowheads indicate membrane ruffling (middle panel) and abnormal cytoplasmic protrusions with the bulbous tips (right panel) in αIIb-W995/β3-transfected CHO cells. Representative images from 3 independent experiments are shown. (H) Abnormal proplatelet formation in αIIb-W995/β3-transfected megakaryocytes. Mouse fetal liver-derived megakaryocytes infected with EGFP-αIIb and Kusabira-Orange-β3 retrovirus were examined in suspension cultures under an IX71 fluorescence microscope with an LCPlanFl 40×/0.60 objective lens (Olympus). (i) The percentage of megakaryocytes extending proplatelets was evaluated manually under a fluorescence microscope 1 to 4 days after infection. For each specimen, at least 100 megakaryocytes were evaluated. The number of proplatelet tips per megakaryocyte (ii) and the size of the proplatelet tips (iii) were measured on acquired images by the ImageScope software Version 10.2.2 (Aperio Technologies). At least 10 megakaryocytes were analyzed for each sample. An unpaired, 2-tailed *t* test was used to analyze data. A value of *P* less than .05 was considered statistically significant. Data are mean plus or minus SD. $^*P < .05$. $^{**}P < .01$. $^{***}P < .0001$. (iv) Representative megakaryocytes from 3 independent experiments are shown. Note that the number of proplatelet tips/bulbous structures (arrowheads) is decreased and the size of the tips increased in αIIb-W995/β3-transfected megakaryocytes than in wild-type αIIb/β3-transfected megakaryocytes. Scale bar represents 10 μm.

Table 1. Platelet characteristics of patients with the *ITGA2B* R995W mutation

Patient	Sex	Age, y	*ITGA2B* mutation	Platelet count, × 10^9/L*	Platelet size, μm†	Surface expression relative to control platelets, %‡					αIIb/β1 tubulin ratio to controls§	Duke bleeding time, minutes‖	Platelet aggregation¶			Bleeding tendency	Initial diagnosis
						αIIb	β3	αIIbβ3	GPIbα	GPIX			ADP, %	Collagen (2.0 μg/mL), %	Ristocetin (1.3 mg/mL), %		
Family 1																	
Patient 1	Male	55	R995W	65	3.9 ± 0.9	53.8	67.0	—	143.1	143.8	0.82	4.5	11 (3μM)	28	77	–	Unknown thrombocytopenia
Family 2																	
Father	Male	46	R995W	79	3.3 ± 0.9	51.3	51.4	56.5	106.7	109.8	—	—	—	—	—	–	—
Patient 2	Male	4	R995W	82	3.6 ± 1.0	54.0	58.6	61.8	138.3	134.7	0.75	5	—	—	—	Epistaxis	Congenital thrombocytopenia
Sister	Female	9	R995W	85	3.4 ± 1.0	55.6	60.6	68.4	120.0	133.1	0.71	3.5	—	—	—	–	—
Family 3																	
Mother	Female	56	R995W	80	2.8 ± 0.8	58.4	63.4	65.8	116.5	—	0.73	—				–	—
Patient 3	Female	27	R995W	74	3.5 ± 1.0	64.4	69.7	63.8	124.8	—	—	—	43 (10μM)	44	72	–	cITP
Sister	Female	24	R995W	100	3.6 ± 1.0	59.3	70.2	70.8	110.9	—	0.63	—	—	—	—	–	—
Family 4																	
Maternal grandfather	Male	58	R995W	66	3.4 ± 0.9	—	—	—	—	—	0.63	—	20 (3μM)	9	—	Hemorrhage in exodontia	—
Mother	Female	30	R995W	66	2.8 ± 0.8	56.3	62.5	57.5	127.2	112.1	0.63	2.5	—	—		Purpura, hemorrhage in exodontia	cITP
Patient 4	Female	4M	R995W	82	3.2 ± 1.0	63.3	62.9	62.3	147.7	140.5	0.63	—	23 (3μM)	11	—	–	NAITP
Brother	Male	5	R995W	122	3.1 ± 0.8	—	—	—	—	—	—	—	—	—	—	–	—
Mean ± SD				81.9 ± 16.8#	3.3 ± 0.3#	57.4 ± 4.4**	62.9 ± 5.8**	63.3 ± 5.0**	126.1 ± 14.3**	129.0 ± 14.5**	0.7 ± 0.07#						

— indicates not applicable; ADP, adenosine diphosphate; cITP, chronic immune thrombocytopenia; and NAITP, neonatal alloimmune thrombocytopenic purpura.

*Controls, 273.5 ± 60.4 (× 10^9/L) (n = 1014).

†Determined by microscopic observation of 200 platelets on a stained peripheral blood smear. Controls, 2.5 ± 0.3 μm (n = 31).

‡Platelets were reacted with fluorescein isothiocyanate-labeled monoclonal antibodies against αIIb (5B12; Dako Denmark), β3 (SZ21), αIIbβ3 (P2), GPIbα (SZ2; Beckman-Coulter), or GPIX (ALMA16; BD Biosciences) and analyzed in an Epics XL flow cytometer (Beckman-Coulter). Values are expressed as percentage of mean fluorescence intensities of control platelets.

§Platelet αIIb/β1-tubulin ratio was determined by densitometric analysis of immunoblots using ImageQuant software Version 5.0 (Molecular Dynamics).

‖Normal range, 2 to 5 minutes.

¶Platelet aggregation was performed in platelet-rich plasma. Results are given as percentage maximum aggregation.

#$P < .001$, **$P < .0001$ vs controls (2-tailed t test).

αIIb-W995/β3-transfected CHO cells exhibited membrane ruffling and abnormal cytoplasmic protrusions with the bulbous tips on fibrinogen-coated surfaces (Figure 1G), indicating that the salt bridge-disrupting mutations exert the same influence on the integrin activation and cytoskeletal events. Abnormal clustering of αIIbβ3, which was reported in *ITGB3* L718P mutation,[10] was not observed in these cells or in platelets spread on immobilized fibrinogen (supplemental Figure 1). It is worth noting that macrothrombocytopenia-associated *ITGB3* mutations in the ectodomain and the cytoplasmic membrane-proximal region have different properties in terms of outside-in signaling and bleeding tendency.[9,10]

Finally, to determine the functional consequences of R995W mutation on platelet production, we coexpressed αIIb and β3 in mouse fetal liver cells by retroviral transfer and differentiated them into megakaryocytes (Figure 1H). There was an early increase and decrease in the percentage of proplatelet formation-positive megakaryocytes in αIIb-W995/β3-transfected megakaryocytes. The number of proplatelet tips was decreased, and the size of the tips increased. These results are consistent with thrombocytopenia and the increased platelet size in patients, indicating that the stimulation of mutant αIIbβ3 leads to abnormal proplatelet formation. However, not all *ITGA2B*- and *ITGB3*-activating mutations are associated with macrothrombocytopenia. Patients with homozygous *ITGB3* C549R or C560R mutation inducing constitutively active αIIbβ3 have a normal platelet count and size,[23,24] suggesting different molecular mechanisms for the induction of abnormal proplatelet formation.

αIIbβ3 has not been implicated in an abnormal platelet count or morphology.[5] Our data support and extend the recent reports that heterozygous, activating mutations in *ITGA2B* and *ITGB3*, in the juxtamembrane region, cause macrothrombocytopenia.[6-10] We thus propose that such mutations represent the etiology of a subset of congenital macrothrombocytopenias. It is also probable that homozygosity causes Glanzmann thrombasthenia, as demonstrated in the original report of macrothrombocytopenia-associated *ITGA2B* R995Q mutation.[6,7] The creation of a knock-in mouse model and/or use of an in vivo megakaryocyte infusion model[25] should clarify the mechanism underlying the production and processing of giant platelets.

Acknowledgments

The authors thank Dr R. C. Mulligan (Children's Hospital Boston, Harvard Medical School, Boston, MA) for 293gp and 293gpg cells, Dr M. Handa (Department of Transfusion Medicine & Cell Therapy, Keio University School of Medicine, Tokyo, Japan) for PT25-2 antibodies, Dr A. Saito (Department of Clinical Research Promotion, Clinical Research Center, National Hospital Organization Nagoya Medical Center) for statistical analysis, and Yoshimi Ito-Yamamura for her skillful technical assistance.

This work was supported by the Japan Society for the Promotion of Science (Grant-in-Aid for Scientific Research), the Ministry of Health, Labor and Welfare, Academic Frontier Project in Japan, Mitsubishi Pharma Research Foundation, the 24th General Assembly of the Japanese Association of Medical Sciences Promotion Fund, the Mother and Child Health Foundation, and the National Hospital Organization Research Fund.

Authorship

Contribution: S.K. designed and performed research, analyzed data, and wrote the paper; H.K. and Y. Tomiyama performed platelet experiments and interpreted the results; M. Onodera constructed retrovirus vectors; M. Otsu, N.T., K.E., and M. Onodera designed the retroviral transfection experiments; Y.M., Y. Takamatsu, J.S., and K.M. contributed patient samples; and H.S. supervised the research.

Conflict-of-interest disclosure: The authors declare no competing financial interests.

Correspondence: Shinji Kunishima, Department of Advanced Diagnosis, Clinical Research Center, National Hospital Organization Nagoya Medical Center, 4-1-1 Sannomaru, Naka-ku, Nagoya 4600001, Japan; e-mail: kunishis@nnh.hosp.go.jp.

References

1. Balduini CL, Cattaneo M, Fabris F, et al. Inherited thrombocytopenias: a proposed diagnostic algorithm from the Italian Gruppo di Studio delle Piastrine. *Haematologica.* 2003;88(5):582-592.
2. Balduini CL, Savoia A. Inherited thrombocytopenias: molecular mechanisms. *Semin Thromb Hemost.* 2004;30(5):513-523.
3. Kunishima S, Saito H. Congenital macrothrombocytopenias. *Blood Rev.* 2006;20(2):111-121.
4. Nurden P, Nurden AT. Congenital disorders associated with platelet dysfunctions. *Thromb Haemost.* 2008;99(2):253-263.
5. Nurden AT. Glanzmann thrombasthenia. *Orphanet J Rare Dis.* 2006;1:10.
6. Hardisty R, Pidard D, Cox A, et al. A defect of platelet aggregation associated with an abnormal distribution of glycoprotein IIb-IIIa complexes within the platelet: the cause of a lifelong bleeding disorder. *Blood.* 1992;80(3):696-708.
7. Peyruchaud O, Nurden AT, Milet S, et al. R to Q amino acid substitution in the GFFKR sequence of the cytoplasmic domain of the integrin IIb subunit in a patient with a Glanzmann's thrombasthenia-like syndrome. *Blood.* 1998;92(11):4178-4187.
8. Ghevaert C, Salsmann A, Watkins NA, et al. A nonsynonymous SNP in the ITGB3 gene disrupts the conserved membrane-proximal cytoplasmic salt bridge in the alphaIIbbeta3 integrin and co-segregates dominantly with abnormal proplatelet formation and macrothrombocytopenia. *Blood.* 2008;111(7):3407-3414.
9. Gresele P, Falcinelli E, Giannini S, et al. Dominant inheritance of a novel integrin beta3 mutation associated with a hereditary macrothrombocytopenia and platelet dysfunction in two Italian families. *Haematologica.* 2009;94(5):663-669.
10. Jayo A, Conde I, Lastres P, et al. L718P mutation in the membrane-proximal cytoplasmic tail of beta3 promotes abnormal alphaIIbbeta3 clustering and lipid microdomain coalescence, and associates with a thrombasthenia-like phenotype. *Haematologica.* 2010;95(7):1158-1166.
11. Kunishima S, Hamaguchi M, Saito H. Differential expression of wild-type and mutant NMMHC-IIA polypeptides in blood cells suggests cell-specific regulation mechanisms in MYH9 disorders. *Blood.* 2008;111(6):3015-3023.
12. Kunishima S, Lopez JA, Kobayashi S, et al. Missense mutations of the glycoprotein (GP) Ibbeta gene impairing the GPIb alpha/beta disulfide linkage in a family with giant platelet disorder. *Blood.* 1997;89(7):2404-2412.
13. Kashiwagi H, Tomiyama Y, Tadokoro S, et al. A mutation in the extracellular cysteine-rich repeat region of the beta3 subunit activates integrins alphaIIbbeta3 and alphaVbeta3. *Blood.* 1999;93(8):2559-2568.
14. Kashiwagi H, Shiraga M, Kato H, et al. Expression and subcellular localization of WAVE isoforms in the megakaryocyte/platelet lineage. *J Thromb Haemost.* 2005;3(2):361-368.
15. Sanuki S, Hamanaka S, Kaneko S, et al. A new red fluorescent protein that allows efficient marking of murine hematopoietic stem cells. *J Gene Med.* 2008;10(9):965-971.
16. Suzuki A, Obi K, Urabe T, et al. Feasibility of ex vivo gene therapy for neurological disorders using the new retroviral vector GCDNsap packaged in the vesicular stomatitis virus G protein. *J Neurochem.* 2002;82(4):953-960.
17. Ory DS, Neugeboren BA, Mulligan RC. A stable human-derived packaging cell line for production of high titer retrovirus/vesicular stomatitis virus G pseudotypes. *Proc Natl Acad Sci U S A.* 1996;93(21):11400-11406.
18. Poncz M, Eisman R, Heidenreich R, et al. Structure of the platelet membrane glycoprotein IIb: homology to the alpha subunits of the vitronectin and fibronectin membrane receptors. *J Biol Chem.* 1987;262(18):8476-8482.

19. Kunishima S, Kobayashi R, Itoh TJ, Hamaguchi M, Saito H. Mutation of the beta1-tubulin gene associated with congenital macrothrombocytopenia affecting microtubule assembly. *Blood.* 2009;113(2):458-461.

20. Hughes PE, Diaz-Gonzalez F, Leong L, et al. Breaking the integrin hinge: a defined structural constraint regulates integrin signaling. *J Biol Chem.* 1996;271(12):6571-6574.

21. Lau TL, Kim C, Ginsberg MH, Ulmer TS. The structure of the integrin alphaIIbbeta3 transmembrane complex explains integrin transmembrane signalling. *EMBO J.* 2009;28(9):1351-1361.

22. Schaffner-Reckinger E, Salsmann A, Debili N, et al. Overexpression of the partially activated alphaIIbbeta3D723H integrin salt bridge mutant downregulates RhoA activity and induces microtubule-dependent proplatelet-like extensions in Chinese hamster ovary cells. *J Thromb Haemost.* 2009;7(7):1207-1217.

23. Mor-Cohen R, Rosenberg N, Peretz H, et al. Disulfide bond disruption by a beta3-Cys549Arg mutation in six Jordanian families with Glanzmann thrombasthenia causes diminished production of constitutively active alphaIIbbeta3. *Thromb Haemost.* 2007;98(6):1257-1265.

24. Ruiz C, Liu CY, Sun QH, et al. A point mutation in the cysteine-rich domain of glycoprotein (GP) IIIa results in the expression of a GPIIb-IIIa (alphaIIbbeta3) integrin receptor locked in a high-affinity state and a Glanzmann thrombasthenia-like phenotype. *Blood.* 2001;98(8):2432-2441.

25. Fuentes R, Wang Y, Hirsch J, et al. Infusion of mature megakaryocytes into mice yields functional platelets. *J Clin Invest.* 2010;120(11):3917-3922.

Table S1. Sequences and locations of oligonucleotide primers used in PCR amplification of *ITGA2B*

Exon	Primers	Sequence	Location	Size (bp)
Promoter	2Bg_p5	GTGCTCAATGCTGTGCCTAC	4112-4131	1,098
	2Bg_p3	GTCCTTGTGGAAGTCCAGTG	5209-5190	
1	2Bg_15	ATTCTAGCCACCATGAGTCC	4868-4887	464
	2Bg_13	CAAGTCACCTTGCTCAACTG	5331-5312	
2 - 4	2Bg_25	ACATCACGGTGGTCTGTGAG	8227-8246	833
	2Bg_43	GAGGCCAGATCCAAAGCAAG	9059-9040	
5 - 7	2Bg_55	CAGCCCTTGCTTTGGATCTG	9035-9054	727
	2Bg_73	TACGAGTCCGCAGTGGAAG	9761-9743	
8 - 12	2Bg_85	TTTCCATCTGCACAATGCAGG	9804-9824	1,369
	2Bg_123	AACTCTCCCATCTGCTCTC	11172-11154	
13 - 18	2Bg_135	CCTGATTGTTAACTCCTGGAG	13281-13301	1,652
	2Bg_183	GGGTTTGGAATGACATCAAGG	14932-14912	
19 - 20	2Bg_195	TTCGTCCTCAGATCTTCTTAC	15666-15686	588
	2Bg_203	TTTGACAGCAAAGCAGAAGAG	16253-16233	
21 - 22	2Bg_215	CACACTAGCATGTGACAGTC	16565-16584	1,105
	2Bg_223	TCCTGACCTCCAGTGATCC	17669-17651	
23 - 26	2Bg_235	AACTTCAGTGTGGCATGCTC	17991-18010	1,073
	2Bg_263	TGCTCCTCCATGTTCACTTG	19063-19044	
27 - 28	2Bg_2755	CATCTCTGGGACTATGTGAG	19202-19221	821
	2Bg_283	CACGTGTCTCCTCAGTCAC	20022-20004	
29	2Bg_285	CAGGAAGAGAGGGAAGGCAAGG	19595-19616	748
	2Bg_2933	ACTCTTGACCTCAGGTGATC	20378-20359	
30	2Bg_305	CAGTGGGCTTCATGTTCTGC	21961-21980	309
	2Bg_303	GAGGGAAACGACACCAAGAG	22269-22250	

The nucleotide positions of primers are based on the sequence of GenBank NG_008331.

Table S2. *ITGA2B* disease haplotype is different in each family

	Family 1	Family 2	Family 3	Family 4
rs56723140 G/C	G	G	G	G
rs990267 G/A	G	G	G	G
rs9900840 C/T	C	C	C	C
rs5910 C/T	**C**	**C**	**T**	**T**
R995W C>T	**T**	**T**	**T**	**T**
rs56311858 C/T	C	C	C	C
NG_008831_22193 C>T	**C**	**C**	**T**	**C**
rs35531721 G/A	G	G	G	G
rs56360368 G/A	G	G	G	G
rs10546679 CT/-	CT	CT	CT	CT
rs850734 G/C	**G**	**C**	**C**	**C**

By cloning and sequencing the PCR products of the ~1.2-kb region flanking the *ITGA2B* R995W mutation, the disease haplotype in each family was defined. Genotypes for the R995W mutation and 10 intragenetic polymorphic sites from the telomere to centromere on chromosome 17q21.32 are shown. The C to T substitution at nucleotide position 22193 of GenBank NG_008331 was not in the SNP database. Informative sites are indicated in bold.

Figure S1. Adhesion of platelets on immobilized fibrinogen

Washed platelets were seeded on 100 μg/ml fibrinogen-coated glass coverslips and incubated for 1 hour at 37°C. Cells were fixed with 3.7% formaldehyde and permeabilized with 0.2% Triton X-100. Coverslips were then stained with anti-CD41a antibody HIP8 followed by Alexa 488-labeled goat anti-mouse IgG.

(A) Representative images from two independent experiments are shown. Scale bar: 20 μm. (B) The area of platelets was measured as the number of pixels per platelet by the ImageJ software (http://rsb.info.nih.gov/ij/). The pixels per platelet were scored, binned, and plotted. Although fully spread platelets were observed (arrow heads), the percentage of poor spread platelets, <0.4 pixels, was increased in the patient. In addition, the average area in the patient was significantly smaller than that of control (the average pixel size, 0.40 ± 0.36 vs. 0.50 ± 0.32, $P<0.05$). Approximately 400 platelets were analyzed in each sample.

Figure S2. Activation state of platelet αIIbβ3 in whole blood

(A) Whole blood from patient 3 diluted in Tyrode's buffer was incubated with FITC-conjugated PAC-1 or FITC-conjugated anti-human fibrinogen antibody (Dako, Glostrup, Denmark) in the presence or absence of 10 μM FK633 or 10 μM ADP and analyzed by flow cytometry. Platelet activation was also assessed employing PE-conjugated CD62p (Beckman-Coulter) in the presence or absence of 200nM PMA. Platelets were discriminated from other blood cells by APC-CD42b (Beckton Dickinson) staining. Numbers indicate the mean fluorescence intensity. Results are representative of two independent experiments. IgG: PE-labeled control IgG1 antibody (Beckman-Coulter). Note that PAC-1 binding to the resting patients' platelets in whole blood is weak compared with that to washed platelets (Figure 1D), suggesting that the procedure of preparing washed platelets may affect the activation state of αIIbβ3.[1] (B) Whole blood from patient 3 was stimulated with various concentrations of ADP, and CD62p expression was assessed. There was no difference between the patient and control in all ADP concentrations. Results are representative of two independent experiments.

REFERENCE

1. Shattil SJ, Cunningham M, Hoxie JA. Detection of activated platelets in whole blood

using activation-dependent monoclonal antibodies and flow cytometry. *Blood.* 1987;70(1):307-315.

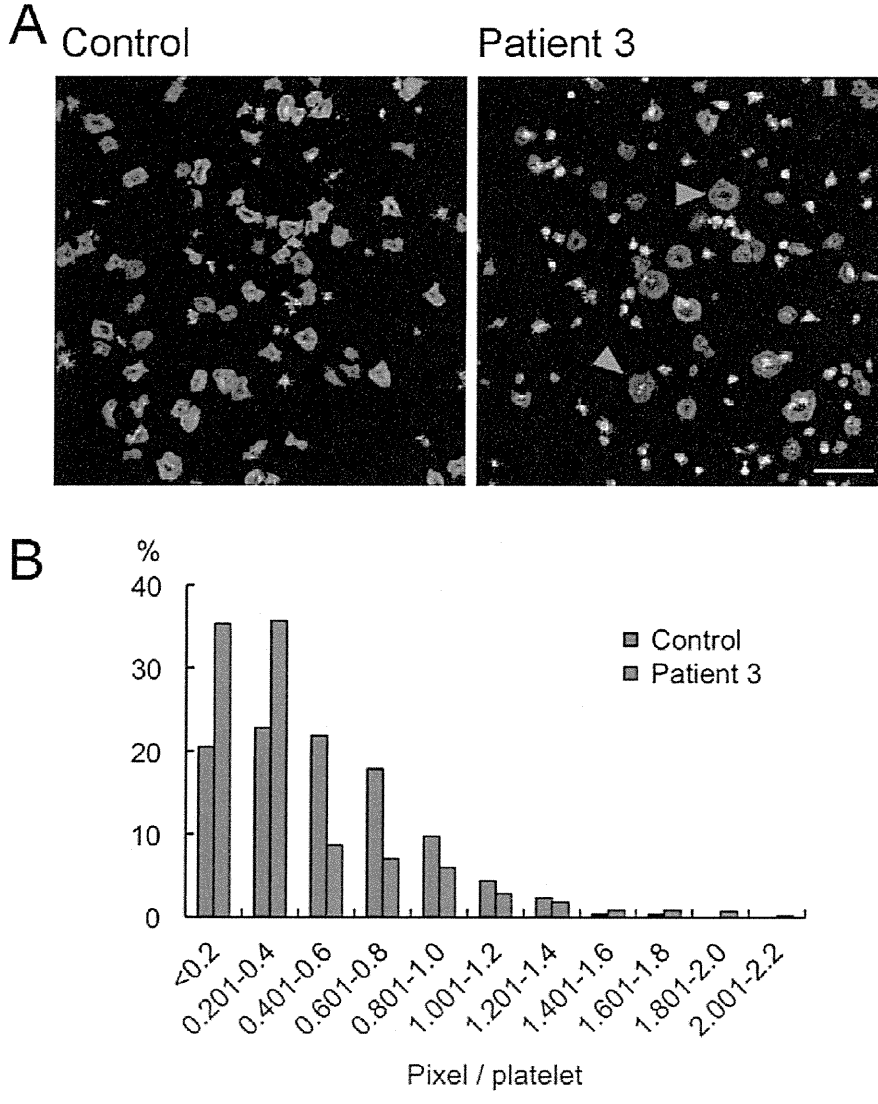
A
Control
Patient 3
B
%
40
30
20
10
0
Control
Patient 3
<0.2
0.201-0.4
0.401-0.6
0.601-0.8
0.801-1.0
1.001-1.2
1.201-1.4
1.401-1.6
1.601-1.8
1.801-2.0
2.001-2.2
Pixel / platelet

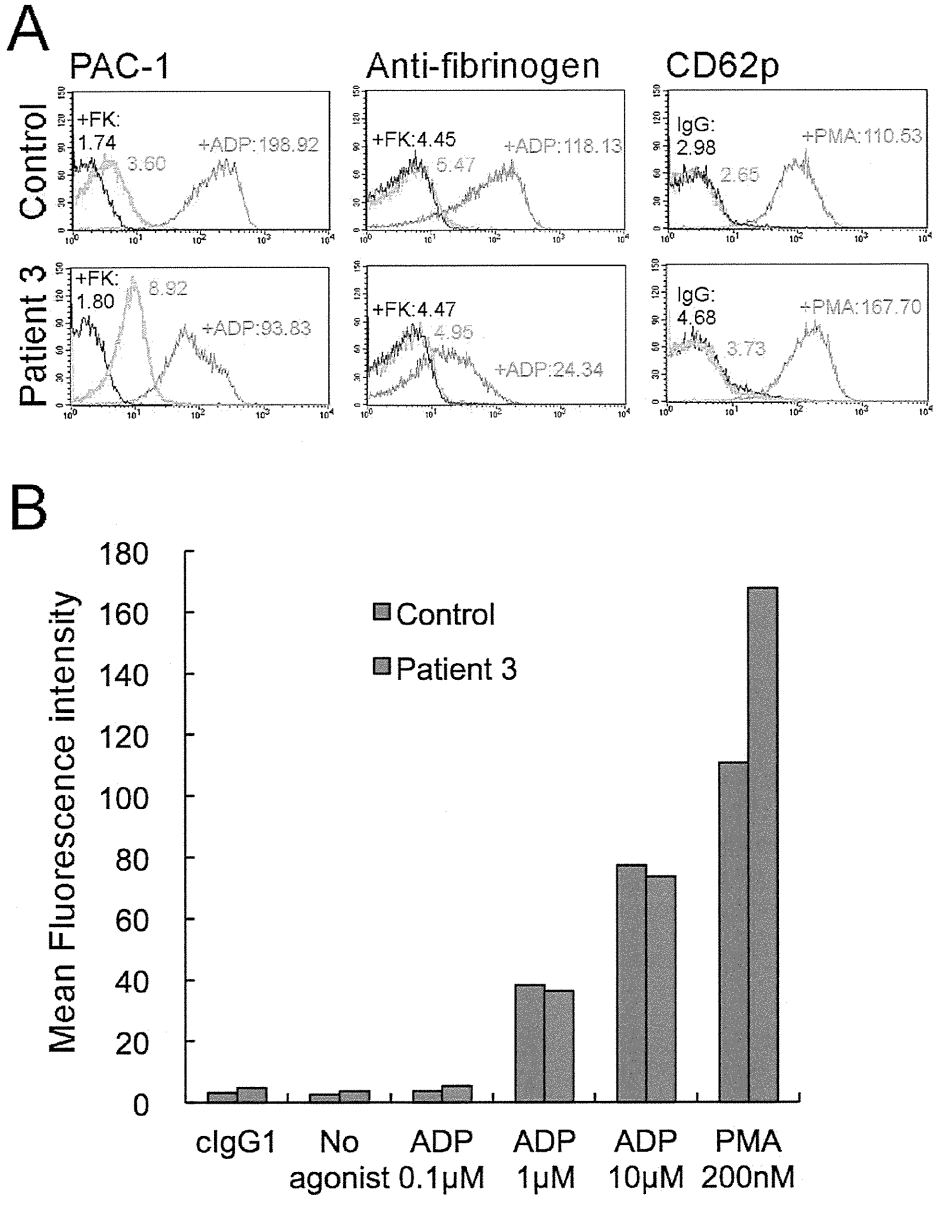
A
PAC-1
Anti-fibrinogen
CD62p
Control
Patient 3
+FK: 1.74
3.60
+ADP:198.92
+FK:4.45
5.47
+ADP:118.13
IgG: 2.98
2.65
+PMA:110.53
+FK: 1.80
8.92
+ADP:93.83
+FK:4.47
4.95
+ADP:24.34
IgG: 4.68
3.73
+PMA:167.70
B
Mean Fluorescence intensity
180
160
140
120
100
80
60
40
20
0
Control
Patient 3
cIgG1
No agonist
ADP 0.1μM
ADP 1μM
ADP 10μM
PMA 200nM

6 Violette EJ, Hardin NJ, McQuillen EN. Sudden unexpected death due to asymptomatic cardiac rhabdomyoma. *J. Forensic. Sci.* 1981; **26**: 599–604.
7 Meissner C, Minnasch P, Gafumbegete E, Reiter A, Gerling I, Oehmichen M. Sudden unexpected infant death due to fibroma of the heart. *J. Forensic. Sci.* 2000; **45**: 731–3.
8 Krous HF, Chadwick AE, Isaacs H Jr. Tumors associated with sudden infant and childhood death. *Pediatr. Dev. Pathol.* 2005; **8**: 20–5.
9 Schenkman KA, O'Rourke PP, French JW. Cardiac rhabdomyoma with cardiac arrest. *West J. Med.* 1995; **162**: 460–2.
10 Somers GR, Smith CR, Perrin DG, Wilson GJ, Taylor GP. Sudden unexpected death in infancy and childhood due to undiagnosed neoplasia: An autopsy study. *Am. J. Forensic. Med. Pathol.* 2006; **27**: 64–9.
11 Burke A, Virmani R. Pediatric heart tumors. *Cardiovasc. Pathol.* 2008; **17**: 193–8.
12 Qin C, Chen L, Xiao YB, Chen BC. Giant primary leiomyoma of the right ventricle. *J. Card. Surg.* 2010; **25**: 169–71.
13 Vural C, Ozen O, Demirhan B. Intravenous lipoleiomyomatosis of uterus with cardiac extension: A case report. *Pathol. Res. Pract.* 2011; **207**: 131–4.
14 Wang JN, Yao CT, Chen JS, Yang YJ, Tsai YC, Wu JM. Cardiac tumors in infants and children. *Acta Paediatr. Taiwan* 2003; **44**: 215–19.

Efficacy of inchinkoto for a patient with liver fibrosis complicated with transient abnormal myelopoiesis in Down's syndrome

Masahiro Takeyama,[1] Yumiko Uchida,[1] Ikuyo Arai,[1] Tomoyuki Kamamoto,[1] Toshiya Nishikubo,[1] Hiromichi Kanehiro,[2] Toshiyuki Sado,[3] Shinji Kunishima[4] and Yukihiro Takahashi[1]

[1]*Division of Neonatal Intensive Care, Center of Maternal Fetal Medicine, Departments of* [2]*Surgery and* [3]*Gynecology, Nara Medical University, Nara and* [4]*Laboratory of Molecular Diagnosis, Department of Advanced Diagnosis, Clinical Research Center, National Hospital Organization Nagoya Medical Center, Nagoya, Japan*

Key words Down's syndrome, liver fibrosis, neonatal, inchinkoto, transient abnormal myelopoiesis.

Transient abnormal myelopoiesis (TAM) is a well-known hematological problem in neonates with Down's syndrome, and is generally considered to spontaneously regress without therapy by the age of 2–3 months.[1] However, it has also been reported that several complications, including liver fibrosis, multiple organ failure and tumor lysis syndrome, lead to poor outcome in some cases.[2,3] Inchinkoto is a Japanese herbal medicine. The drug has recently been used for postoperative biliary atresia patients.[4] We report herein a neonate with Down's syndrome who developed liver fibrosis as a complication of TAM and was treated with inchinkoto.

Case Report

An infant was born to a 40-year-old primigravida. Prenatal ultrasound at 32 weeks detected fetal pericardial effusion and hepatomegaly. At 33 weeks of gestation, cesarean section was performed due to hydrops fetalis and fetal bradycardia. The infant was male with features of Down's syndrome. Birth weight was 2076 g. Apgar scores were 8 and 9 at 1 and 5 min, respectively. Laboratory test results are shown in Table 1. Peripheral white blood cell (WBC) count was 221 600/μL with 85% blasts. Findings on peripheral blood smear were consistent with TAM. Umbilical cord blood cytogenesis showed 47, XY, +21, and GATA-1 mutation was confirmed in blast cells from umbilical cord blood. He showed newborn respiratory distress syndrome and had to be intubated on postnatal day 1, and was ventilated for 9 days. No cardiac anomalies were noted. At birth, elevated serum concentrations of lactate dehydrogenase, total and indirect bilirubin, and transaminase were noted, and serum markers for liver fibrosis, hyaluronic acid (<50 ng/mL) and type IV collagen (<150 ng/mL) showed high levels. Furthermore, hemorrhage diathesis developed. Thus, Down's syndrome with TAM and liver fibrosis was diagnosed. The clinical course is shown in Figure 1. Repeated substitution of fresh frozen plasma and anti-thrombin III resulted in improvement of hemorrhagic diathesis. The patient was treated with cytarabine (1 mg/kg/day for 5 days). Following these treatments, WBC count was decreased and blasts disappeared. Hyaluronic acid levels were also decreased. However, bilirubin levels continued to gradually increase (3.1 mg/dL) and type IV collagen levels remained high (1038 mg/dL). Liver biopsy was performed on postnatal day 30. Histological changes in the liver showed predominantly pericellular and perisinusoidal fibrosis, associated with perivenular fibrosis. Furthermore, α-smooth-muscle-actin-(SMA)-positive myofibroblast-like cells and CD42b-positive atypical cells were seen (Fig. 2). Based on the results of liver biopsy, he was treated with the Japanese herbal medicine inchinkoto (0.15 g/kg/day) (Tsumura & Co., Tokyo, Japan) on postnatal day 46. Direct bilirubin was decreased promptly (2.0 mg/dL) on postnatal day 71. He was diagnosed with

Correspondence: Masahiro Takeyama, MD, PhD, Division of Neonatal Intensive Care Unit, Center of Maternal Fetal Medicine, Nara Medical University, 840 Shijo-cho, Kashihara, Nara 634-8522, Japan. Email: mtake@naramed-u.ac.jp

Received 10 April 2010; revised 8 November 2010; accepted 26 January 2011.
doi: 10.1111/j.1442-200X.2011.03365.x

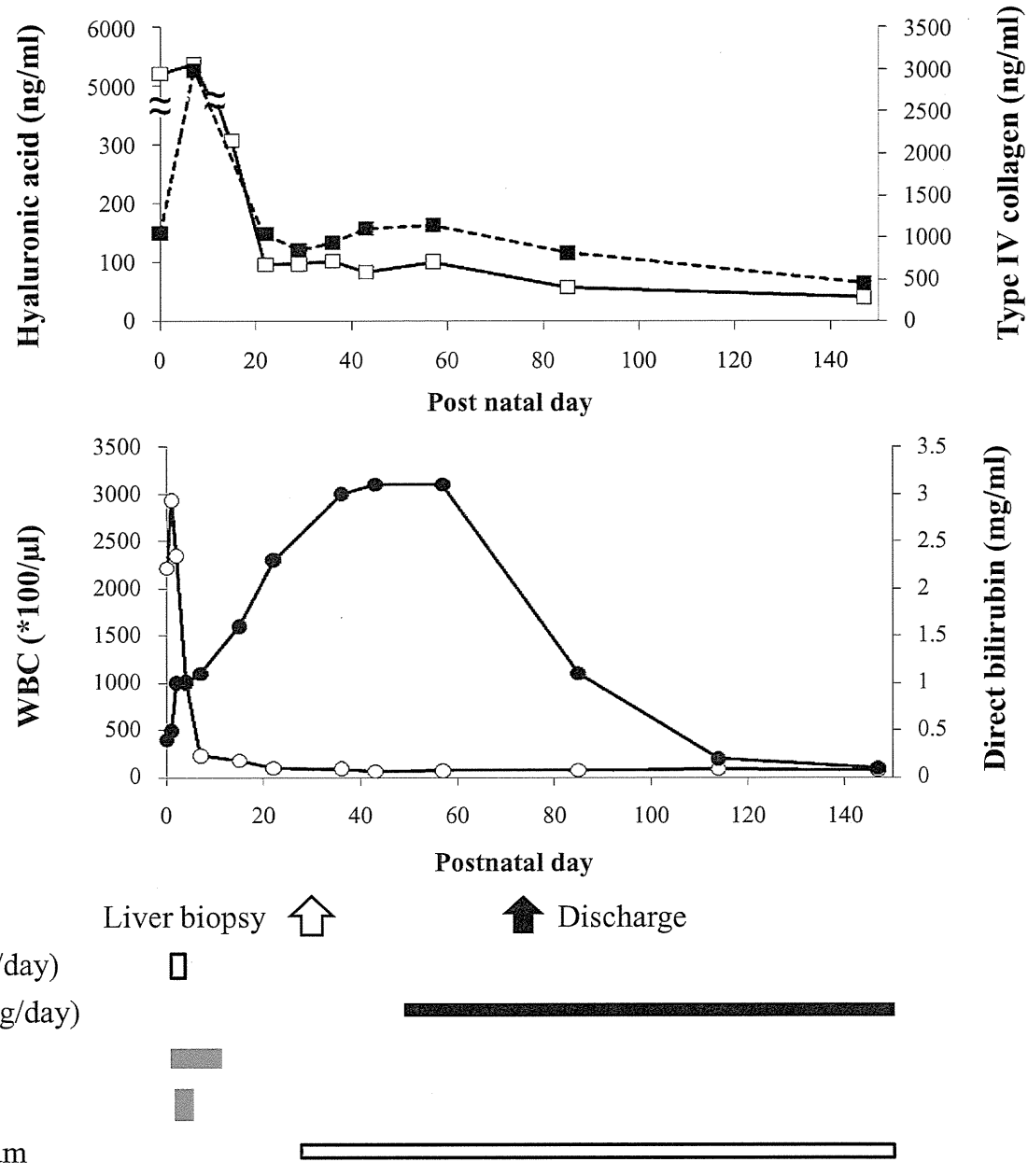

Fig. 1 Clinical course. Solid circles, direct bilirubin (mg/dL); open circles, white blood cells (WBC, *100/μl); solid squares, type IV collagen (ng/mL); open squares, hyaluronic acid (ng/mL).

hypothyroidism on a mass-screening test and was given levothyroxine sodium on postnatal day 23. The patient was discharged on postnatal day 75. At 5 months and 6 days, hyaluronic acid, type IV collagen levels and direct bilirubin had decreased to 40.5 ng/mL, 458 ng/mL and 0.1 mg/dL, respectively.

Discussion

Down's syndrome is a common congenital disorder affecting approximately 1/1000 live births, and TAM occurs in about 10% of newborns with Down's syndrome. Recently, mutations in the gene encoding the hematopoietic growth factor GATA-1 have been shown to be specific for TAM and AMKL in Down's syndrome.[5] Our case had the GATA-1 mutation Q17X (69C>T), causing a lack of expression of the full-length GATA-1 protein.[6] TAM has thus been regarded as a benign disease. However, in some cases, the disease is severe and can result in death due to multiple organ failure and/or liver failure. In this case, the patient had hepatomegaly during the fetal period. This indicates liver fibrosis from at least 32 weeks of gestation. The cause of liver fibrosis remains unclear. Miyauchi *et al.*[7] proposed that abnormal blasts in TAM and cytokines can induce hepatic fibrosis. Multiple clinical markers, including types III and IV collagen, hyaluronic acid and N-terminal propeptide of collagen III, may be useful for non-invasive measurement of liver fibrosis. In our patient, hyalu-

Table 1 Laboratory findings

Peripheral blood		Blood chemistry		Serological tests		Coagulation studies		Markers of liver fibrosis		Flow cytometry (umbilical cord blood)
RBC	3.98×10^6 /μl	TP	4.4 g/dL	IgG	392 mg/dL	PT	63.4 s (10–15 s)	Type IV collagen	1053 ng/mL	CD41 (45.2%) with co-expression of CD61 (46.4%) and CD42b (24.8%)
Hb	15.1 g/dL	Alb	2.9 g/dL	IgA	<2 mg/dL	APTT	>180 s (25–50 s)	Hyaluronic acid	5214 ng/mL	
Ht	44%	AST	82 IU/L	IgM	4 mg/dL	Fib	103 mg/dL			
MCV	110.6 fl	ALT	79 IU/L			HPT	25%			
MCH	37.9 pg	LDH	4188 IU/L			AT-III	<20%			
MCHC	34.3%	BUN	8 mg/dL			D-dimer	2.0 μg/mL			
WBC	221 660 /μl	Cr	0.6 mg/dL							
Myelo	2%	Na	137 mEq/L							
Meta	1%	K	4.5 mEq/l							
Stab	0%	Ca	8.9 mg/dL							
Seg	2%	T.Bil	3.7 mg/dL							
Eos	3%	D.Bil	0.4 mg/dL							
Bas	0%	I.Bil	3.3 mg/dL							
Lym	6%	CRP	0.9 mg/dL							
Mono	1%									
Blast	85%									
Plt	183×10^3/μl									

Alb, albumin; ALT, alanine aminotransferase; APTT, activated partial thromboplastin time; AST, aspartate aminotransferase; AT-III, antithrombin-III; Bas, basophil; BUN, blood urea nitrogen; CD, cluster of differentiation; Cr, creatinine; CRP, C-reactive protein; D.Bil, direct bilirubin; Eos, eosinophil; Fib, fibrinogen; Hb, hemoglobin; HPT, hepaplastin test; Ht, hematocrit; I.Bil, indirect bilirubin; Ig, immunoglobulin; LDH, lactate dehydrogenase; Lym, lymphocyte; MCH, mean corpuscular hemoglobin; MCHC, mean corpuscular hemoglobin concentration; MCV, mean corpuscular volume; Meta, metamyelocyte; Mono, monocyte; Myelo, myelocyte; Plt, platelets; PT, prothrombin time; RBC, red blood cell; Seg, segmented neutrophil; Stab, stab cell; T.Bil, total bilirubin; TP, total protein; WBC, white blood cell count.

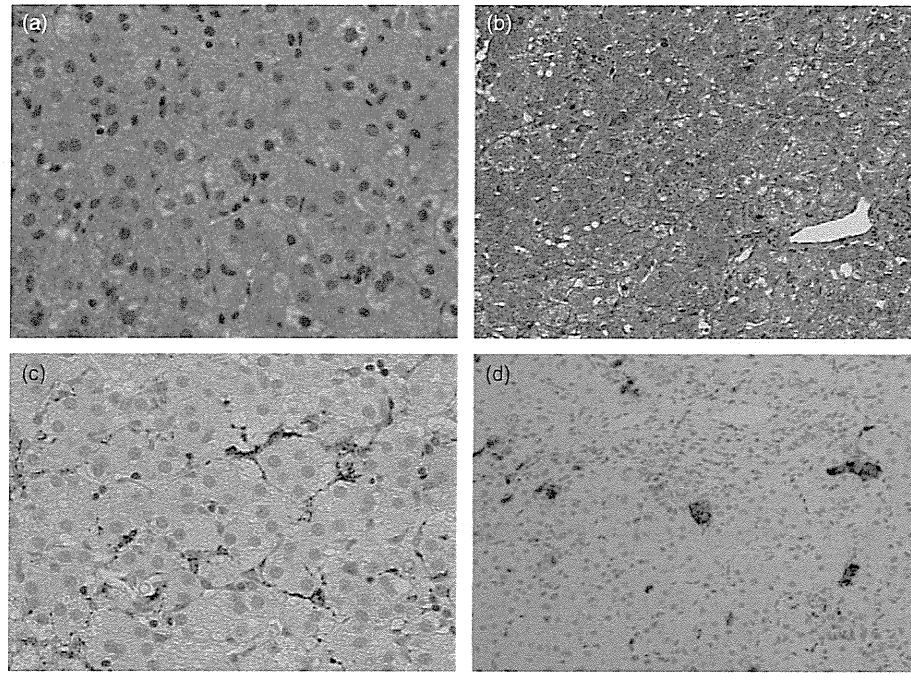

Fig. 2 Histological findings of liver biopsy. (a) Ballooning of hepatocytes with cholestasis is seen (hematoxylin–eosin stain, ×400). (b) Predominantly pericellular and perisinusoidal fibrosis, associated with perivenular fibrosis are seen (Azan staining, ×200). (c) α-smooth-muscle-actin-positive myofibroblast-like cells are seen in sinusoidal areas on immunohistochemical study (×400). (d) CD42b-positive megakaryocytes are seen in fibrotic or sinusoidal areas on immunohistochemical study (×200).